

# Revisiting and Maximizing Temporal Knowledge in Semi-supervised Semantic Segmentation

Wooseok Shin, Hyun Joon Park, Jin Sob Kim, Sung Won Han



**Abstract**—In semi-supervised semantic segmentation, the Mean Teacher- and co-training-based approaches are employed to mitigate confirmation bias and coupling problems. However, despite their high performance, these approaches frequently involve complex training pipelines and a substantial computational burden, limiting the scalability and compatibility of these methods. In this paper, we propose a PrevMatch framework that effectively mitigates the aforementioned limitations by maximizing the utilization of the temporal knowledge obtained during the training process. The PrevMatch framework relies on two core strategies: (1) we reconsider the use of temporal knowledge and thus directly utilize previous models obtained during training to generate additional pseudo-label guidance, referred to as previous guidance. (2) we design a highly randomized ensemble strategy to maximize the effectiveness of the previous guidance. Experimental results on four benchmark semantic segmentation datasets confirm that the proposed method consistently outperforms existing methods across various evaluation protocols. In particular, with DeepLabV3+ and ResNet-101 network settings, PrevMatch outperforms the existing state-of-the-art method, Diverse Co-training, by +1.6 mIoU on Pascal VOC with only 92 annotated images, while achieving 2.4 times faster training. Furthermore, the results indicate that PrevMatch induces stable optimization, particularly in benefiting classes that exhibit poor performance. Code is available at <https://github.com/wooseok-shin/PrevMatch>.

**Index Terms**—Consistency regularization, semantic segmentation, semi-supervised learning, temporal knowledge

## 1 INTRODUCTION

SEMANTIC segmentation [1]–[4] is a critical task in various computer vision-related applications, such as autonomous driving [5]–[7], medical image analysis [8], [9], robotics [10], among others [11]–[13], where the goal is to assign a semantic class label to each pixel in an image. Despite the recent success of supervised learning-based methods in semantic segmentation, obtaining precise pixel-level annotations for supervised learning is extremely time-consuming and expensive. This limits the applicability of supervised learning-based methods across various domains and fields. Thus, extensive research has been conducted in semi-supervised semantic segmentation to overcome this limitation. The research has focused on developing methods enabling models to learn effectively from a limited number of labeled images along with a large number of unlabeled images.

In semi-supervised learning, self-training [14]–[21] and consistency regularization [22]–[33] have become the predominant approaches for utilizing unlabeled data. In particular, self-training involves generating pseudo-labels using the predictions of the current model at each iteration for unlabeled samples and leveraging them to train the model in conjunction with labeled data. Consistency regularization encourages a network to predict consistently for various perturbed forms of identical input. Recent studies have focused on designing frameworks that combine self-training and consistency regularization to exploit the strengths of each method. However, self-training-based methods still suffer from the confirmation bias problem [17] even when combined with consistency regularization.

This problem is attributed to the accumulation of pseudo-label errors produced by the model itself, which exacerbate as self-training progresses. To mitigate this problem, existing methods distinguish the model prediction processes for supervised outputs and pseudo-labels. In other words, the supervised outputs and pseudo-labels are obtained from different predictions, respectively. Among them, some studies [32], [34], [35] have adopted the weak-to-strong consistency paradigm from the perspective of input separation, which supervises the prediction from a strongly perturbed input using the pseudo-label generated from its weakly perturbed counterpart (Fig. 1a). Its success is based on the idea that more reliable pseudo-labels can be derived from weak perturbations, and strong perturbations aid in mitigating confirmation bias [17], [21], broadening the knowledge and unlabeled data space [29], [32], [36], and shifting the model’s decision boundary to low-density regions [37]. Because of this advantage, the weak-to-strong consistency paradigm has become a fundamental component of the most recent methods.

Another method to obtain different prediction views involves using network perturbation based on a teacher-student structure. In particular, Mean Teacher [26] is a representative approach in semi-supervised segmentation, where a teacher network is derived using an exponential moving average (EMA) of the student model’s weights (Fig. 1b). Although the Mean Teacher generates somewhat different prediction views between the teacher and student, this method is limited by a coupling problem [27]: as training progresses, the teacher and student become tightly linked, and consequently, the teacher’s predictions become similar to those of the student. To mitigate the coupling problem

Wooseok Shin, Hyun Joon Park, Jin Sob Kim, and Sung Won Han are with the School of Industrial and Management Engineering, Korea University, Seoul, Republic of Korea.

Corresponding author: Sung Won Han ([swhan@korea.ac.kr](mailto:swhan@korea.ac.kr))

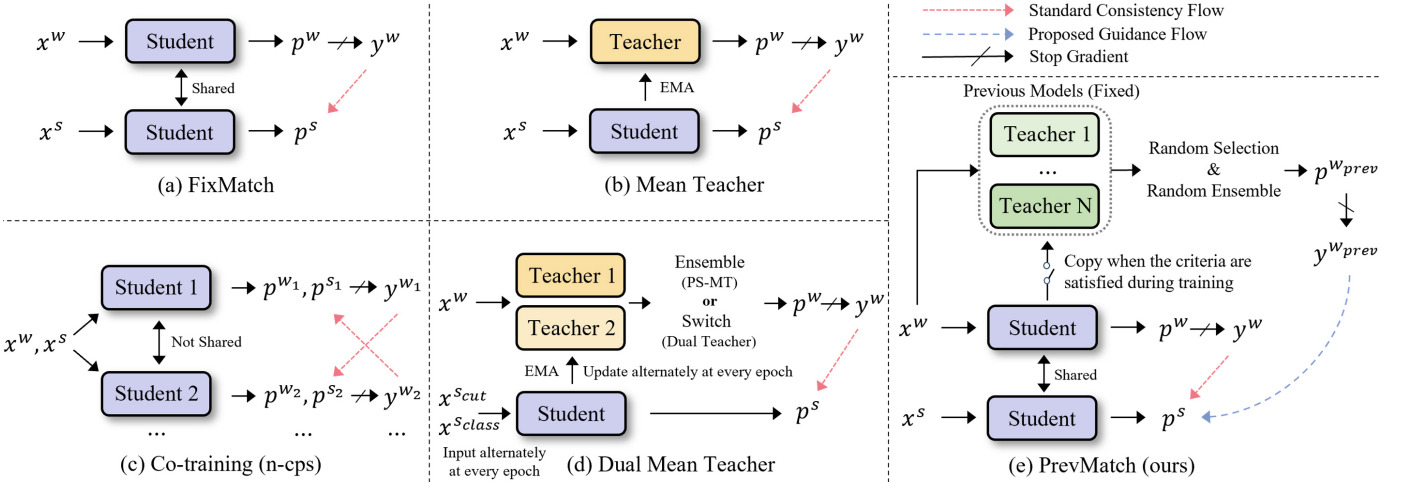


Fig. 1. Illustration of the frameworks for (a) FixMatch [34] (or PseudoSeg [35]), (b) Mean Teacher-based structure [26], [38]–[40], (c) Co-training [28], [29] (cps: cross pseudo supervision), (d) Dual Mean Teacher [30], [31], and (e) the proposed method. In (d), the inputs ( $x^{s_{cut}}$ ,  $x^{s_{class}}$ ) indicate the CutMix [41] and ClassMix [42] augmentations used in Dual Teacher [31].

and obtain diverse predictions, certain studies [30], [31] have proposed a dual EMA teacher-based framework where two teachers are alternately updated at every epoch (Fig. 1d). Among them, PS-MT [30] produces more reliable pseudo-labels by ensembling the predictions of the two teachers. By contrast, Na et al. [31] reported that ensembling predictions can reduce the diversity of pseudo-labels. Thus, they proposed a Dual Teacher framework that alternately activates two teachers in each epoch to generate diversified pseudo-labels. Although these studies have demonstrated the benefits of using multiple teachers to mitigate the coupling problem, their ability to provide reliable and diverse pseudo-labels simultaneously remains limited. In addition, they have incorporated additional complex components to ensure diversity between the two teachers. In particular, adversarial feature perturbation and a new loss function are used for PS-MT. Further, distinct types of augmentation provided to each teacher (e.g., CutMix or ClassMix) and layer perturbation are used for Dual Teacher. Consequently, this complexity can hinder the scalability and compatibility of these approaches with existing semi-supervised methods.

Instead of using EMA-based teachers, a co-training paradigm [27]–[29], [43]–[47] has been widely used to expand prediction views (Fig. 1c). This paradigm involves simultaneously training multiple networks with different initializations in a mutual teaching manner, where each network supervises the others using pseudo-labels generated from its predictions. Building on this concept, subsequent studies [29], [45] have demonstrated that increasing the diversity of pseudo-label views from student networks improves their generalization ability. For example, this can involve the use of more co-networks, diverse input domains (e.g., RGB and frequency), or different architectures (e.g., CNN and Transformer). Co-training provides diverse pseudo-label guidance with stability and without concerns regarding the coupling problem. However, its scalability remains constrained due to computational complexity and resource demands.

In this paper, we propose the PrevMatch framework, which efficiently expands pseudo-label views by maximiz-

ing the utilization of previous models obtained during training, as depicted in Fig. 1e. The PrevMatch framework is based on two main ideas. First, to efficiently address the coupling problem, we revisit the utilization of temporal knowledge. Specifically, we save several models at specific epochs during training and utilize their predictions as additional guidance, referred to as *previous guidance*, which acts as a regularizer in conjunction with standard guidance. This strategy addresses the coupling problem and reduces the complexity associated with additional training components. Second, we design a highly randomized ensemble strategy to maximize the effectiveness of utilizing the previous guidance. This approach involves selecting a random number of models from those previously saved and ensembling their predictions using randomized weights. This strategy can efficiently provide diverse and reliable pseudo-labels, while avoiding the significant computational complexity inherent in co-training approaches.

Extensive experiments conducted across various evaluation protocols on the PASCAL, Cityscapes, COCO, and ADE20K datasets reveal that the proposed PrevMatch significantly outperforms existing methods. In particular, compared to Diverse Co-training, the current state-of-the-art method, PrevMatch achieves a +1.6 mIoU improvement on Pascal VOC with 92 labels while accelerating training by 2.4 times. In addition to quantitative evaluations, ablation studies and analyses of the proposed components are conducted to explain the success of PrevMatch.

## 2 RELATED WORK

### 2.1 Semi-supervised Learning

The central challenge in semi-supervised learning lies in extracting additional supervision for unlabeled samples. Previous studies can be categorized into two main approaches: self-training and consistency regularization. Self-training-based methods [14]–[20] assign pseudo-labels to unlabeled data using the ongoing model predictions and integrate them with labeled data to retrain the model. Consistency regularization methods [22]–[27], [34], [43], [48], [49] enforce

a model to produce invariant predictions for different perturbations, such as input and network perturbations.

In terms of input perturbations [22]–[25], [34], [48], the  $\Pi$ -model [22], [23], [50] applies simple stochastic perturbations, while VAT [24] applies adversarial perturbations to unlabeled samples. Subsequently, UDA [25] expands the perturbation pool using RandAugment [51] to provide diverse augmented samples. Furthermore, FixMatch [34], a standard approach in recent semi-supervised learning, adopts a weak-to-strong paradigm where the prediction for a strongly perturbed input is supervised by pseudo-labels generated from the prediction for a weakly perturbed input. Network perturbation, another approach to enforcing consistency regularization, has also been widely investigated [23], [26], [27], [43], [49]. Temporal Ensembling [23] and Mean Teacher [26] methods leverage earlier predictions and weights of the model, respectively, to obtain different prediction views. In addition, co-training-based methods [27], [43], [49] adopt multiple networks with different initializations and enforce consistency regularization between their predictions. Among the numerous studies discussed, the weak-to-strong paradigm, Mean Teacher structure, and co-training approaches have been widely used to advance semi-supervised semantic segmentation.

## 2.2 Semi-supervised Semantic Segmentation

Owing to the detailed nature of the segmentation task, which involves numerous pixels and multiple classes within an image, semantic segmentation requires more time-consuming and costly efforts to annotate labels and demands sophisticated approaches for accurate performance. Thus, recent research has increasingly focused on developing methods for semi-supervised semantic segmentation, based on previous achievements in semi-supervised learning. Early studies [52], [53] employed a GAN framework [54] to generate additional supervision for unlabeled images by distinguishing between pseudo-labels and manual labels. Recent studies have focused on developing improved methods based on weak-to-strong consistency, Mean Teacher, and co-training paradigms. PseudoSeg [35] adopts a weak-to-strong paradigm based on a single network. CPS [28], [45] and GCT [55] employ two networks for co-training and demonstrate that co-training outperforms the Mean Teacher approach. Subsequent studies have integrated the weak-to-strong paradigm (i.e., input perturbation) into the Mean Teacher or co-training approaches (i.e., network perturbation), demonstrating performance improvements.

A stream of research that combines the weak-to-strong paradigm with the Mean Teacher structure has proposed techniques such as advanced data augmentation [38]–[40], [56], prototype learning [57], curriculum learning [58], symbolic reasoning [59], and dual Mean Teacher [30], [31]. Among them, PS-MT [30] and Dual Teacher [31] methods implement a dual EMA teacher-based framework to mitigate the coupling problem between the teacher and student models, with two teachers alternately updating each epoch based on the EMA of the student’s weights. However, their pipelines inevitably involve complex components to resolve the coupling problem, limiting the scalability and compatibility of these approaches. Moreover, regarding pseudo-label generation, PS-MT ensembles the predictions of two

teachers to improve reliability, whereas Dual Teacher alternately uses the predictions of each teacher to enhance diversity. However, neither method satisfies both reliability and diversity. In other words, PS-MT improves the reliability of pseudo-labels but lacks diversity, whereas Dual Teacher suffers from the opposite limitation.

Another stream of research, combining the weak-to-strong paradigm with co-training, has developed techniques such as a shared backbone with multiple heads [46], conservative-progressive learning [60], and increasing the diversity of co-training [29]. Among them, Li et al. [29] investigated the working mechanism of co-training and discovered that providing distinct pseudo-label views improves generalization ability. To this end, they proposed Diverse Co-training, which incorporates variations in the input domains (RGB and frequency) and architectures (CNN and Transformer). However, in diverse co-training, the number of whole networks to train increases as pseudo-label views increase.

In this study, instead of using Mean Teacher or co-training approaches, we revisit the utilization of temporal knowledge and efficiently expand pseudo-label views by maximizing the use of previous models. The proposed PrevMatch framework can be seen as simplifying and extending [30], [31] while also enhancing the efficiency of [29]. Specifically, we eliminate the complex components used in [30], [31], such as distinct augmentation types for each epoch, layer/adversarial feature perturbations, EMA teachers, and a new loss function. Instead, PrevMatch reuses the previous models and the weakly perturbed input used in the standard flow, thereby improving the simplicity and compatibility of the overall framework. Furthermore, we provide reliable and diverse pseudo-labels to the student network through a highly randomized ensemble strategy. Moreover, although both PrevMatch and co-training provide diverse pseudo-label views, PrevMatch operates on a single trainable network with fixed previous models. This facilitates greater efficiency in terms of computational and memory costs.

## 2.3 Temporal Knowledge in Semi-supervised Learning

In the context of semi-supervised learning, several studies have leveraged temporal knowledge obtained from previous training stages. Temporal Ensembling [23] accumulates predictions for unlabeled samples across different epochs using the EMA approach and enforces consistency between the current and EMA predictions. Mean Teacher [26] averages the model weights across the training steps using the EMA approach, producing a more stable teacher network. As a further extension, a dual EMA teacher-based framework was proposed [30], [31], where two teachers are alternately updated at each epoch. Moreover, TC-SSL [20] measures the time-consistency (TC) scores of individual samples across training epochs and selects unlabeled samples with higher TC scores for consistency learning. This approach assumes that time-consistent predictions are typically accurate. Similar to TC-SSL, ST++ [21] proposes a selective re-training scheme that selects more reliable samples based on a stability score. The stability score based on the mIoU metric is derived from comparisons between

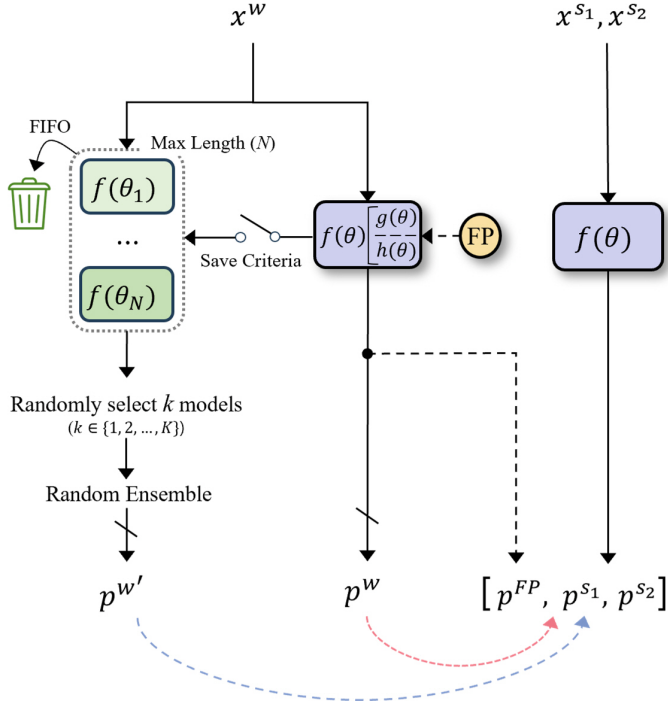


Fig. 2. Overall framework of PreVMatch (based on UniMatch). FP indicates the feature perturbation used in UniMatch.  $g$  and  $h$  are the encoder and decoder of the entire network  $f$ , respectively. When the maximum length of the previous list is exceeded, the oldest model is replaced with the new model using a first-in-first-out (FIFO) approach. The red and blue arrows denote standard and proposed guidance flows, respectively.

the predictions of the final model and those of several checkpoints obtained during training. In addition to semi-supervised learning, Feng et al. [61] proposed a temporal consistency framework that adopts two temporary teachers to learn instance temporal consistency in representation learning.

### 3 METHOD

This section describes the preliminaries and overall training flow for semi-supervised semantic segmentation. The PreVMatch method is also introduced here.

#### 3.1 Preliminaries & Overall Workflow

Semi-supervised semantic segmentation aims to fully utilize unlabeled images  $D_u = \{x_i^u\}$ , given only a limited number of labeled images  $D_l = \{(x_i^l, y_i^l)\}$ . In general semi-supervised learning, the objective function is divided into supervised loss  $L_s$  and unsupervised loss  $L_u$  as follows:

$$L = \frac{1}{2}(L_s + L_u). \quad (1)$$

1. **Supervised Flow** In supervised flow, a segmentation network  $f$  receives a labeled image  $x^l$  and generates the corresponding predicted class distribution  $p^l$ . Subsequently, the supervised loss is calculated using pixel-wise cross-entropy  $H$  between the prediction and the ground-truth label. This can be formulated as follows.

$$L_s = \sum_{i,j} H(y_{ij}^l, p_{ij}^l), \quad (2)$$

where  $i$  and  $j$  indicate pixel indices.

2. **Unsupervised – Standard Flow** Following the success of the weak-to-strong consistency paradigm popularized by FixMatch [34], most semi-supervised segmentation methods have adopted this paradigm. Concretely, two perturbed images (i.e.,  $x^w$  and  $x^s$ ) are obtained by applying weak and strong augmentations to an unlabeled image  $x^u$ . The network  $f$  receives the two perturbed images and outputs the predicted class distributions  $p^w$  and  $p^s$ . As there is no ground-truth label for the unlabeled image, a pseudo-label for the weakly perturbed prediction is obtained by:  $y^w = \text{argmax}(p^w)$ . Then, this pseudo-label is used to supervise the strongly perturbed prediction, as depicted in the standard flow presented in Fig. 1e (red arrow). This consistency term can be formulated as follows.

$$C(p^w, p^s) = \sum_{i,j} \mathbb{1}(\max(p_{ij}^w) \geq \tau) H(y_{ij}^w, p_{ij}^s), \quad (3)$$

where  $\mathbb{1}(\cdot)$  is an indicator function, and  $\tau$  is a confidence threshold used to ignore noise in a pseudo-label. Furthermore, the UniMatch framework [32] introduced two contributions based on FixMatch: the dual stream image-level perturbation and the feature-level perturbation strategies, to expand the perturbation space, thereby achieving significant improvements. Therefore, we select the UniMatch framework as our baseline. In particular, two strongly perturbed images ( $x^{s1}$  and  $x^{s2}$ ) are derived by randomly applying a strong augmentation pool to the same image,  $x^u$ . Subsequently, their corresponding predictions ( $p^{s1}$  and  $p^{s2}$ ) are generated through the network  $f$ . Regarding the feature-level perturbation strategy, the prediction is obtained as follows:  $p^{fp} = h(\text{Dropout}(g(x^w)))$ , where  $g$  and  $h$  are the encoder and decoder of the entire network  $f$ , respectively. Ultimately, three predictions are simultaneously supervised by a common pseudo-label derived from a weak view (red arrow in Fig. 2). This can be formulated as follows.

$$L_{u(\text{standard})} = C(p^w, p^{s1}) + C(p^w, p^{s2}) + C(p^w, p^{fp}). \quad (4)$$

3. **Unsupervised – Proposed Flow** To obtain additional pseudo-label guidance, the same weakly perturbed image,  $x^w$ , used in the standard branch, is fed into the previous model branch. Subsequently,  $k$  models, where  $k$  is chosen randomly from  $\{1, 2, \dots, K\}$ , are selected from the saved list of previous models, and  $k$  predictions for  $x^w$  are generated. Previous guidance,  $p^{w'}$ , is obtained by aggregating the  $k$  predictions using randomized ensemble weights to improve the diversity of the pseudo-label view. As illustrated by the blue arrow in Fig. 2, the previous guidance functions as additional regularizers, supervising the three predictions. This can be formulated as follows.

$$L_{u(\text{prev})} = C(p^{w'}, p^{s1}) + C(p^{w'}, p^{s2}) + C(p^{w'}, p^{fp}). \quad (5)$$

Finally, the total loss of the unsupervised flow is defined by combining the standard and proposed flow losses as

follows:

$$L_u = L_{u(\text{standard})} + \lambda \cdot L_{u(\text{prev})}, \quad (6)$$

where  $\lambda$  denotes the weight of the proposed flow.

### 3.2 Previous Guidance: Revisiting Temporal Knowledge

To address the coupling problem between student and teacher networks, we revisit the utilization of temporal knowledge that can be obtained during the training process. In the literature, Temporal Ensembling [23] and Mean Teacher [26] methods average the temporal knowledge of a model in terms of its predictions and weights, respectively. PS-MT [30] and Dual Teacher [31], inheriting the spirit of the Mean Teacher [26] method, aim to further exploit temporal knowledge by adopting two EMA teachers. TC-SSL [20] and ST++ [21] methods implement a filtering mechanism to exclude less-informative unlabeled samples using specific scoring criteria measuring temporal consistency.

In contrast to existing methods, we directly utilize previous models and generate pseudo-label guidance from their predictions without relying on a complex pipeline of dual EMA-based methods or a filtering mechanism. In particular, we store multiple models at different epochs that meet the specified criteria during training and use their pseudo-labels as additional guidance, referred to as previous guidance. As training progresses, the decoupling between the student and previously saved teachers increases, allowing for the acquisition of different prediction views. However, as decoupling becomes more pronounced, the positive effects of self-training from correct pseudo-labels may diminish due to the use of outdated teachers. Therefore, previous guidance is used in conjunction with the standard guidance obtained from the current student. In addition, we define the maximum length ( $N$ ) of the list for storing previous models and replace the oldest teacher with a newer one when this limit is exceeded to avoid using excessively outdated teachers. Formally, one previous model is randomly selected from the previous model list  $\{T_1, T_2, \dots, T_N\}$ . Then, this model processes the same weakly perturbed image,  $x^w$ , used in the standard flow and produces predictions  $p^{w'}$ . The previous guidance is obtained by:  $y^{w'} = \text{argmax}(p^{w'})$ , and it supervises three predictions according to Eq. (5). In this way, we produce diverse pseudo-labels, as in prior studies [28]–[31], by leveraging different previous models encompassing varied perspectives of temporal knowledge, without complex additional components or heavy computational burden.

**Save Criteria.** In this approach, storing the appropriate previous models is crucial for generating diverse and reliable pseudo-labels. Some studies [21], [62], [63] that employ intermediate models for ensembling or filtering in image recognition and segmentation save the model at regular intervals (e.g., every 20 epochs in a total of 100 epochs). By contrast, we save the model when it achieves the best performance on the validation set to ensure the stability of the previous guidance. The weights and performances of the neural network can vary significantly during the optimization process, and excessively large fluctuations may increase negative impacts. These negative impacts can be exacerbated by label scarcity and a pronounced class imbalance in semi-supervised semantic segmentation compared

to standard image recognition. In addition, the periodic saving method requires additional hyperparameter searches to determine appropriate intervals. Therefore, we adopt our saving approach to achieve stability and simplicity (refer to Table 9 for related experiments).

The efficacy of the previous guidance can be intuitively explained as follows. When using only standard guidance, two training scenarios arise based on whether the prediction is correct or incorrect. In cases where the prediction is incorrect, the network is trained in the wrong direction. In contrast, given the standard and previous guidance, four scenarios can be considered based on whether they are correct or incorrect (standard-previous): (1) correct-correct, (2) correct-incorrect, (3) incorrect-correct, and (4) incorrect-incorrect. Through case (3), the network receives an additional opportunity to be guided in the right direction, away from the wrong one. Although model training may be hindered through case (2), leading to significant fluctuations, we empirically demonstrate that the positive effects of the proposed method outweigh the negative effects (which is further supported by the analysis of training stability in Section 4.4.1). In addition, previous guidance can help mitigate the network’s catastrophic forgetting problem [64], [65], where previously learned knowledge is forgotten when acquiring new knowledge. In particular, this phenomenon can be more pronounced in self-training and class-imbalance scenarios (i.e., in our scenario) due to the lack of labeled data, potentially leading to significant performance fluctuations in poorly behaved classes [19]. In semi-supervised [20] and representation learning [61], some studies have demonstrated that utilizing temporal knowledge helps mitigate the catastrophic forgetting problem and stabilizes training. Based on this fact, we explore the learning stability of the proposed method in Section 4.4.1.

### 3.3 Maximizing Efficacy of Previous Guidance

One way to improve the reliability of the predictions involves using network ensemble techniques. These techniques have been widely used in various domains as a promising method for improving performance. In particular, several studies [62], [63] in the field of image recognition have demonstrated that ensembles of multiple intermediate models obtained during training also improve prediction accuracy and diversity. Therefore, we utilize network ensembling to improve the reliability of the previous guidance. In designing this method, we also consider computational complexity and pseudo-label diversity. To this end, given the list that includes  $N$  previous models, we randomly select  $K$  ( $K \leq N$ ) models for each iteration to mitigate the increase in computational complexity while ensuring pseudo-label diversity. However, this approach, which always ensembles  $K$  models, may not guarantee the diversity of pseudo-labels, as noted in Dual Teacher [31]. This problem can worsen for large values of  $K$ .

Therefore, to provide reliable and diverse pseudo-labels to the student network, we propose a highly randomized ensemble strategy comprising the following two ideas:

- **Random Selection:** For each iteration, we randomly select a varying number of teachers,  $k$ , ranging from 1 to  $K$ . For example,  $k=1, 2$ , or 3 can be selected for each iteration when  $K=3$ . With this approach, selecting a large

$k$  tends to yield consistent pseudo-labels, enhancing reliability, while a small  $k$  contributes to increased diversity in the pseudo-labels. In addition, computational costs are lower than those incurred when using a fixed number  $K$ . This strategy enables the student network to obtain stable and diverse guidance, which functions as a robust regularizer, aiding network optimization.

- **Random Weights:** Regarding ensemble weights, we propose a random aggregation strategy that averages  $k$  predictions using random weights for each iteration instead of a simple average of  $k$  predictions. In particular, the  $k$  selected teachers receive  $x^w$  and output  $k$  predictions,  $\{p_1^{w'}, p_2^{w'}, \dots, p_k^{w'}\}$ . The final previous guidance is then obtained by aggregating these predictions using random weights as follows:

$$p^{w'} = \sum_{i=1}^k w_i \cdot p_i^{w'}, \quad (7)$$

where  $w_i$  is derived from a Dirichlet distribution as follows:  $\{w_1, w_2, \dots, w_k\} \sim \text{Dir}(\alpha_1, \alpha_2, \dots, \alpha_k)$ . Note that the sum of  $w_i$  is one. This approach explores all combinations of previous guidance in a continuous space, expanding the original pseudo-label space beyond a simple average.

In this way, the proposed randomized ensemble strategy can improve the reliability and diversity of the previous guidance while mitigating the increase in computational complexity.

## 4 EXPERIMENTS

### 4.1 Experimental Configuration

#### 4.1.1 Datasets

**PASCAL VOC** [66] is a widely used benchmark dataset in semantic segmentation, comprising 21 distinct categories (20 object types and a background class). This dataset contains 10,582 images designated for training purposes, segmented into two subsets based on annotation quality: 1,464 images constitute the high-quality subset, characterized by detailed annotations, whereas the remaining 9,118 images form the coarse subset, featuring less detailed annotations. This study follows established protocols for a fair comparison [28], [32], [39], [67]. In particular, three training protocols are considered based on the criteria for selecting labeled images.

- **Original:** A protocol whereby labeled images are exclusively sourced from the high-quality subset.
- **Blended:** A protocol that entails a random selection of labeled images from the total dataset.
- **Priority:** A protocol where the selection of labeled images is first derived from the high-quality subset; if not sufficient, it is complemented by additional images from the coarse subset.

**Cityscapes** dataset [68], tailored for the semantic analysis of urban street scenes, comprises 2,975 high-resolution images for training and 500 images for validation, primarily focusing on 19 categories within urban environments. Consistent with previous studies [21], [29], [32], we evaluate this dataset using various label partitions, specifically 1/16, 1/8, 1/4, and 1/2 of the total number of labels.

**COCO** dataset [69], notable for its complexity and scale, comprises 118k training and 5k validation images. This dataset features dense annotations across 81 classes set in various indoor and outdoor scenarios. Considering the performance plateaus observed in datasets such as Pascal and Cityscapes and the higher number of classes, the COCO dataset has emerged as a practical and valuable benchmark for evaluating advanced algorithms in semi-supervised segmentation. Following existing studies [32], we validate the proposed method using 1/256, 1/128, and 1/64 label partitions.

**ADE20K** dataset [70], containing more diverse scenes and a greater number of classes (150 categories) than COCO, comprises 20,210 images for training and 2,000 images for validation. Using the label partitions from existing studies [33], we evaluate the proposed method on 1/128, 1/64, and 1/32 partitions.

In all protocols, training images not selected as labeled images are utilized as unlabeled images.

#### 4.1.2 Architecture and Implementation Details

Consistent with existing literature, we employ ResNet-50 and ResNet-101 backbones [71] as encoders for the Pascal VOC, Cityscapes, and ADE20K datasets. For the COCO dataset, Xception-65 [72] is adopted as the backbone. We use DeepLabV3+ [3] as the segmentation head and set its output stride to 16 for efficient training.

For the training setups, each mini-batch comprises 8 labeled and 8 unlabeled images. The proposed method is trained for 80, 240, 30, and 40 epochs for the PASCAL, Cityscapes, COCO, and ADE20K datasets, respectively, using the SGD optimizer. The learning rates are initially set to 0.001, 0.005, 0.004, and 0.004 for these datasets, respectively, and are managed using a polynomial learning rate scheduler. Moreover, we use 321/513, 801, 513, and 513 random crops for these datasets, respectively. For image augmentation, we use common weak (e.g., resize, crop, and flip) and strong (e.g., color transformations, grayscale, cutmix, and blur) data augmentations, as in UniMatch [32]. For the hyperparameters of standard consistency flow,  $\tau$  is set to 0 for Cityscapes and 0.95 for the other datasets. The dropout rate for feature perturbation is set to 0.5.

For the hyperparameters of PrevMatch,  $\tau$  is set to 0.9 for Pascal, 0 for Cityscapes, and 0.95 for COCO and ADE20K. The maximum length ( $N$ ) of the previous list is set to eight for Pascal and Cityscapes and five for COCO and ADE20K. The upper bound number  $K$  for the random selection is set to three. For weight  $\lambda$ , as previous guidance should correct the model before it becomes overfitted in the wrong direction (i.e., confirmation bias [17]) during the middle of training, setting an appropriate weight  $\lambda$  is crucial. Additionally, as the initial model typically exhibits poor performance, we implement a warmup schedule for the weight of the proposed flow, similar to the commonly used polynomial learning rate scheduler that includes a warmup phase. Experiments are conducted in the following environments: UBUNTU 20.04, Python 3.10.4, PyTorch 1.12.1, CUDA 11.3, and NVIDIA RTX 3090Ti or A6000 GPUs. The training is performed using one GPU for Pascal and two GPUs for the other datasets.

TABLE 1

Comparison with state-of-the-art methods on the *Original* protocol of Pascal VOC dataset. The numeric values in the header (e.g., 92) represent the number of labeled images used for training. All methods are trained using ResNet-50/101 and DeepLabV3+. The number of trainable whole networks and input resolution are reported. The values of PrevMatch are averaged over three runs. The evaluation metric is the mean IoU (%).

Pascal [Original set]	Encoder	#Trainable Networks	Resolution	# Labeled images (Total: 10582)					
				92	183	366	732	1464	
Supervised Baseline		R-50	×1	513 <sup>2</sup>	44.0	52.3	61.7	66.7	72.9
PseudoSeg [35]	[ICLR'21]	R-50	×1	513 <sup>2</sup>	54.9	61.9	64.9	70.4	71.0
PC <sup>2</sup> Seg [73]	[ICCV'21]	R-50	×1	513 <sup>2</sup>	56.9	64.6	67.6	70.9	72.3
CPCL [60]	[TIP'23]	R-50	×2	512 <sup>2</sup>	61.9	67.0	72.1	74.3	-
AugSeg [39]	[CVPR'23]	R-50	×1	512 <sup>2</sup>	64.2	72.2	76.2	77.4	78.8
UniMatch [32]	[CVPR'23]	R-50	×1	321 <sup>2</sup>	71.9	72.5	76.0	77.4	78.7
Dual Teacher [31]	[NeurIPS'23]	R-50	×1	321 <sup>2</sup>	70.8	74.5	76.4	77.7	78.2
PrevMatch (ours)	—	R-50	×1	321 <sup>2</sup>	<b>73.4</b>	<b>75.4</b>	<b>77.5</b>	<b>78.6</b>	<b>79.3</b>
Supervised Baseline		R-101	×1	513 <sup>2</sup>	45.1	55.3	64.8	69.7	73.5
CPS [28]	[CVPR'21]	R-101	×2	512 <sup>2</sup>	64.1	67.4	71.7	75.9	-
ReCo [74]	[ICLR'22]	R-101	×1	321 <sup>2</sup>	64.8	72.0	73.1	74.7	-
PS-MT [30]	[CVPR'22]	R-101	×1	512 <sup>2</sup>	65.8	69.6	76.6	78.4	80.0
ST++ [21]	[CVPR'22]	R-101	×1	321 <sup>2</sup>	65.2	71.0	74.6	77.3	79.1
U <sup>2</sup> PL [67]	[CVPR'22]	R-101	×1	512 <sup>2</sup>	68.0	69.2	73.7	76.2	79.5
GTA-Seg [75]	[NeurIPS'22]	R-101	×2	513 <sup>2</sup>	70.0	73.2	75.6	78.4	80.5
PCR [57]	[NeurIPS'22]	R-101	×1	513 <sup>2</sup>	70.1	74.7	77.2	78.5	80.7
DGCL [76]	[CVPR'23]	R-101	×1	513 <sup>2</sup>	70.5	77.1	78.7	79.2	81.6
CCVC [47]	[CVPR'23]	R-101	×2	512 <sup>2</sup>	70.2	74.4	77.4	79.1	80.5
iMAS [40]	[CVPR'23]	R-101	×1	513 <sup>2</sup>	68.8	74.4	78.5	79.5	81.2
AugSeg [39]	[CVPR'23]	R-101	×1	512 <sup>2</sup>	71.1	75.5	78.8	80.3	81.4
UniMatch [32]	[CVPR'23]	R-101	×1	321 <sup>2</sup>	75.2	77.2	78.8	79.9	81.2
ESL [58]	[ICCV'23]	R-101	×1	513 <sup>2</sup>	71.0	74.1	78.1	79.5	<b>81.8</b>
LogicDiag [59]	[ICCV'23]	R-101	×1	513 <sup>2</sup>	73.3	76.7	77.9	79.4	-
LogicDiag + MKD [59]	[ICCV'23]	R-101	×2	513 <sup>2</sup>	74.7	77.2	78.4	80.1	-
Diverse Co-T. (2-cps) [29]	[ICCV'23]	R-101	×2	321 <sup>2</sup>	74.8	77.6	79.5	80.3	81.7
Diverse Co-T. (3-cps) [29]	[ICCV'23]	R-101	×3	321 <sup>2</sup>	75.4	76.8	<b>79.6</b>	<b>80.4</b>	81.6
PrevMatch (ours)	—	R-101	×1	321 <sup>2</sup>	<b>77.0</b>	<b>78.5</b>	<b>79.6</b>	<b>80.4</b>	81.6

TABLE 2

Comparison with state-of-the-art methods on the *Blended* protocol of Pascal VOC dataset. All methods are trained using ResNet-50 and DeepLabV3+. The fractional values indicate the ratio of labeled images used for training.

Pascal [Blended set]	Resolution	1/16	1/8	1/4	
Supervised Baseline	513 <sup>2</sup>	62.4	68.2	72.3	
Mean Teacher [26]	[NeurIPS'17] 512 <sup>2</sup>	66.8	70.8	73.2	
CCT [44]	[CVPR'20] 512 <sup>2</sup>	65.2	70.9	73.4	
GCT [55]	[ECCV'20] 512 <sup>2</sup>	64.1	70.5	73.5	
CutMix-Seg [38]	[BMVC'20] 512 <sup>2</sup>	68.9	70.7	72.5	
CAC [77]	[CVPR'21] 320 <sup>2</sup>	70.1	72.4	74.0	
CPS [28]	[CVPR'21] 512 <sup>2</sup>	72.0	73.7	74.9	
UCC [46]	[CVPR'22] 512 <sup>2</sup>	74.1	74.8	76.4	
PS-MT [30]	[CVPR'22] 512 <sup>2</sup>	72.8	75.7	76.4	
UniMatch [32]	[CVPR'23] 321 <sup>2</sup>	74.5	75.8	76.1	
AugSeg [39]	[CVPR'23] 512 <sup>2</sup>	74.7	76.0	77.2	
iMAS [40]	[CVPR'23] 513 <sup>2</sup>	74.8	76.5	77.0	
CCVC [47]	[CVPR'23] 512 <sup>2</sup>	74.5	76.1	76.4	
PrevMatch (ours)	—	321 <sup>2</sup>	75.6	76.4	76.3
		513 <sup>2</sup>	<b>76.0</b>	<b>77.1</b>	<b>77.6</b>

## 4.2 Comparison with State-of-the-Art Methods

**PASCAL VOC.** Three main experiments are conducted on the *Original*, *Blended*, and *Priority* protocols, which are

TABLE 3

Comparison with state-of-the-art methods on the *Priority* protocol of Pascal VOC dataset. All methods are trained using ResNet-101 and DeepLabV3+.

Pascal [Priority set]	Resolution	1/16	1/8	1/4	
Supervised Baseline	513 <sup>2</sup>	70.6	75.0	76.5	
U <sup>2</sup> PL [67]	[CVPR'22] 512 <sup>2</sup>	77.2	79.0	79.3	
UniMatch [32]	[CVPR'23] 513 <sup>2</sup>	80.9	<b>81.9</b>	80.4	
AugSeg [39]	[CVPR'23] 512 <sup>2</sup>	79.3	81.5	80.5	
Dual Teacher [31]	[NeurIPS'23] 513 <sup>2</sup>	80.1	81.5	80.5	
PrevMatch (ours)	—	513 <sup>2</sup>	<b>81.4</b>	<b>81.9</b>	<b>80.8</b>

divided according to the criteria for selecting labeled images. In Table 1, the proposed method outperforms state-of-the-art methods in almost all partitions, even with a single trainable network and a lower resolution. In particular, PrevMatch significantly improves performance in settings with fewer labels (92 and 183). Compared to Diverse Co-T, PrevMatch exhibits comparable performance in settings with more than 366 labels, but it operates on a single trainable network, indicating that the proposed method is efficient with respect to training costs. For *Blended* and *Priority* protocols reported in Tables 2 and 3, the proposed method consistently outperforms existing methods.

TABLE 4

Comparison with state-of-the-art methods on the Cityscapes dataset. All methods are trained using ResNet-50/101 and DeepLabV3+.

Cityscapes		Encoder	#Trainable Networks	1/16 (186)	1/8 (372)	1/4 (744)	1/2 (1488)
Supervised Baseline		R-50	×1	63.3	70.2	73.1	76.6
PS-MT [30]	[CVPR'22]	R-50	×1	-	75.8	76.9	77.6
U <sup>2</sup> PL [67]	[CVPR'22]	R-50	×1	70.6	73.0	76.3	77.2
UniMatch [32]	[CVPR'23]	R-50	×1	75.0	76.8	77.5	78.6
iMAS [40]	[CVPR'23]	R-50	×1	74.3	77.4	78.1	<b>79.3</b>
AugSeg [39]	[CVPR'23]	R-50	×1	73.7	76.5	<b>78.8</b>	<b>79.3</b>
CCVC [47]	[CVPR'23]	R-50	×2	74.9	76.4	77.3	-
FPL (w/ CPS) [78]	[CVPR'23]	R-50	×2	74.8	77.3	78.5	-
Diverse Co-T. (3-cps) [29]	[ICCV'23]	R-50	×3	-	76.5	77.9	-
PrevMatch (ours)	—	R-50	×1	<b>75.8</b>	<b>77.8</b>	<b>78.8</b>	79.2
Supervised Baseline		R-101	×1	66.3	72.8	75.0	78.0
CPS [28]	[CVPR'21]	R-101	×2	69.8	74.3	74.6	76.8
AEL [56]	[NeurIPS'21]	R-101	×1	75.8	77.9	79.0	80.3
PS-MT [30]	[CVPR'22]	R-101	×1	-	76.9	77.6	79.1
U <sup>2</sup> PL [67]	[CVPR'22]	R-101	×1	74.9	76.5	78.5	79.1
PCR [57]	[NeurIPS'22]	R-101	×1	73.4	76.3	78.4	79.1
CISC-R [79]	[TPAMI'23]	R-101	×1	-	75.9	77.7	-
FPL (w/ AEL) [78]	[CVPR'23]	R-101	×1	76.6	78.2	78.5	-
AugSeg [39]	[CVPR'23]	R-101	×1	75.2	77.8	79.6	80.4
UniMatch [32]	[CVPR'23]	R-101	×1	76.6	77.9	79.2	79.5
ESL [58]	[ICCV'23]	R-101	×1	75.1	77.2	78.9	<b>80.5</b>
UPC (w/ U <sup>2</sup> PL) [80]	[ICCV'23]	R-101	×1	75.3	77.4	79.0	79.6
Diverse Co-T. (2-cps) [29]	[ICCV'23]	R-101	×2	75.0	77.3	78.7	-
Diverse Co-T. (3-cps) [29]	[ICCV'23]	R-101	×3	75.7	77.4	78.5	-
Dual Teacher [31]	[NeurIPS'23]	R-101	×1	76.8	78.4	79.5	<b>80.5</b>
PrevMatch (ours)	—	R-101	×1	<b>77.7</b>	<b>78.9</b>	<b>80.1</b>	80.1

**Cityscapes.** Experimental results for the Cityscapes validation set are listed in Table 4. Under four label partitions using ResNet-50 and ResNet-101 backbones, the proposed method outperforms previous methods in six out of eight cases. Similar to the results reported in Table 1, PrevMatch consistently improves performance in setups with fewer labels. However, certain methods (e.g., AugSeg, AEL, and Dual Teacher) perform better than PrevMatch at the 1/2 label setups. This can be attributed to the advanced data augmentation techniques used in these methods. In other words, these methods could achieve better performance because the 1/2 label partition increasingly resembles a supervised learning setting, where augmentation techniques play a crucial role. Thus, we intend to explore the efficacy of the advanced augmentations on the proposed method in future work.

**COCO & ADE20K.** Table 5 lists results for the large-scale datasets COCO and ADE20K. The proposed method consistently improves the performance across all partitions compared to the baseline, UniMatch, suggesting that PrevMatch is also effective on large-scale datasets.

### 4.3 Ablation Studies

In the ablation studies and discussion, the baseline refers to the UniMatch method [32].

TABLE 5

Evaluation results on the large-scale datasets using Xception-65 for COCO and ResNet-50 for ADE20K.

Method	COCO			ADE20K		
	1/256	1/128	1/64	1/128	1/64	1/32
Supervised	28.0	33.6	37.8	7.2	9.9	13.7
UniMatch [32]	38.9	44.4	48.2	13.6	18.3	23.9
PrevMatch (ours)	<b>40.2</b>	<b>45.7</b>	<b>48.4</b>	<b>15.4</b>	<b>19.6</b>	<b>24.9</b>

#### 4.3.1 Individual Efficacy of the Proposed Components

The effects of the individual components are investigated, and the results are presented in Table 6. The first row indicates the baseline. All components of the proposed method consistently achieve performance gains. In particular, previous guidance, which randomly selects one previous model from the previous list for each iteration to generate additional guidance, surpasses the baseline by 0.8% and 1.3% in the 92- and 183-label settings, respectively. Regarding the number of models ( $K$ ) for the network ensemble, we experiment with simple ensemble (fixed  $K$ ) or random selection (random  $K$ ) strategies. The result (third row) obtained using fixed  $K$  exhibits minor performance gains. In contrast, the results using random  $K$  (fourth row) indicate significantly improved performance. This implies that a fixed  $K$  ensemble improves the reliability of pseudo-labels but limits the diversity, as noted in Dual Teacher



TABLE 6

Ablation study of the components of the proposed method using a ResNet-50 encoder. For the ensemble, we set  $K=3$ . The means and standard deviation are also reported based on three runs to validate statistical significance.

Previous Guidance	Simple Ensemble	Random Selection	Random Weights	PASCAL	
				92	183
-	-	-	-	71.9 $\pm$ 0.5	72.5 $\pm$ 0.7
✓	-	-	-	72.7 $\pm$ 0.5	73.8 $\pm$ 0.6
✓	✓	-	-	72.7 $\pm$ 0.4	74.1 $\pm$ 0.5
✓	-	✓	-	73.2 $\pm$ 0.4	74.9 $\pm$ 0.6
✓	-	✓	✓	<b>73.4<math>\pm</math>0.4</b>	<b>75.4<math>\pm</math>0.5</b>

TABLE 7

Ablation study for the maximum length of the previous list using a ResNet-50 encoder. In this setting, only previous guidance is used (i.e.,  $K=1$ , without ensemble).

List Length ( $N$ )	Base.	1	2	4	8	12	20
Pascal <sub>92</sub>	71.9	71.7	71.7	72.4	<b>72.7</b>	72.5	71.9
Pascal <sub>183</sub>	72.5	72.7	72.9	73.4	<b>73.8</b>	73.5	73.3

[31], whereas a random  $K$  strategy can provide reliable and diverse guidance to the model. In addition, using random weights for network ensembling contributes to performance gains, indicating that it expands the original pseudo-label space by generating diversified guidance.

#### 4.3.2 Previous List Length

We investigate the effect of the length ( $N$ ) of the previous list that stores the temporal models. In Table 7, the results for  $N = 1$  and  $N = 2$  are comparable to those of the baseline. This suggests that the aforementioned coupling problem may persist because the previous models in the list are continually updated with the latest model when  $N$  is small. The cases of  $N = 4, 8$ , and  $12$  consistently outperform the baseline, revealing that the proposed method is not highly sensitive to hyperparameters. However, the performance for  $N = 20$  increases only marginally due to the use of outdated teachers. Based on this result, we recommend setting the value of  $N$  to approximately 5–15% of the total training epochs, which proves to be appropriate for different datasets (e.g., Pascal=6–10, Cityscapes=8–16, and COCO and ADE20k=4–5).

#### 4.3.3 Upper Bound Number for Random Selection

To generate reliable and diverse pseudo-labels, we proposed a strategy that randomly selects  $k$  models (ranging from 1 to  $K$ ) for each iteration. In this strategy, we explore the performance changes regarding the upper bound number  $K$ . Table 8 indicates that including the ensembling cases ( $K > 1$ , i.e.,  $k=1$  or  $k > 1$  are randomly selected) improves the performance significantly compared to the case of  $K = 1$  (i.e., without ensemble). In addition, we observe the best results at  $K = 3$  and a slight performance drop in settings with  $K$  greater than 3. Even for large  $K$ , a varying number ( $k$ ) of models is selected; however, the proportion of large  $k$  values increases with  $K$ . This ensures consistent pseudo-labels but reduces their diversity, potentially degrading performance, as mentioned in Dual Teacher [31]. In conclusion,

TABLE 8

Ablation study on the efficacy of the upper bound number  $K$  using a ResNet-50 encoder and  $N=8$ .

Upper Bound Number ( $K$ )	1	2	3	4	5
Pascal <sub>92</sub>	72.7	73.1	<b>73.4</b>	<b>73.4</b>	73.1
Pascal <sub>183</sub>	73.8	74.9	<b>75.4</b>	75.2	75.1

TABLE 9

Ablation study regarding the efficacy of the save criteria using a ResNet-50 encoder,  $N=8$ , and  $K=3$ .

Save Criteria	92	183	366	732	1464
(a) Baseline	71.9	72.5	76.0	77.4	78.7
(b) Every 1 Epoch	71.8	73.5	76.3	77.5	78.6
(c) Every 3 Epochs	72.2	74.7	76.8	78.0	78.6
(d) On Best Epochs (PrevMatch)	<b>73.4</b>	<b>75.4</b>	<b>77.5</b>	<b>78.6</b>	<b>79.3</b>

we select  $K = 3$  because it adequately satisfies the diversity and reliability requirements of the pseudo-labels.

#### 4.3.4 Criteria for Saving Previous Models

As described in Section 3.2, one alternative for storing previous models involves saving the model at regular intervals, a method used in [21], [62], [63]. Thus, we conduct experiments to validate the effectiveness of this approach. As listed in Table 9, although case (b) exhibits slightly better overall performance than the baseline (a), the difference is marginal. This suggests that storing models at short intervals does not address the coupling problem between the teacher and student networks. In contrast, case (c) shows a significant improvement compared to case (a). Although case (c) functions well, it exhibits limited improvements compared to case (d) which utilizes the proposed save criteria, demonstrating the superiority of the proposed approach. In addition, our approach does not require additional hyperparameter searches to determine appropriate intervals, thereby reducing unnecessary training costs.

## 4.4 Discussion

### 4.4.1 Analysis of Performance and Training Stability

**Class-wise IoU Scores and Qualitative Evaluation.** Tables 10 and 11 list the category-wise IoU scores. In particular, Table 10 on Pascal VOC shows that the proposed method achieves notable performance gains for the chair and sofa classes, which were particularly challenging for the UniMatch baseline. In addition, Table 11 on the Cityscapes dataset shows that the proposed method achieves the largest performance improvements for the wall, fence, and terrain classes, which are the lowest performing among the 19 classes in UniMatch. In addition to the quantitative results, the qualitative results shown in Fig. 3 corroborate these findings, revealing consistent improvements in the same categories. Thus, these results suggest that utilizing previous knowledge helps prevent the catastrophic forgetting problem described in Section 3.2, even in semi-supervised semantic segmentation scenarios. We further investigate this problem in the subsequent analysis.

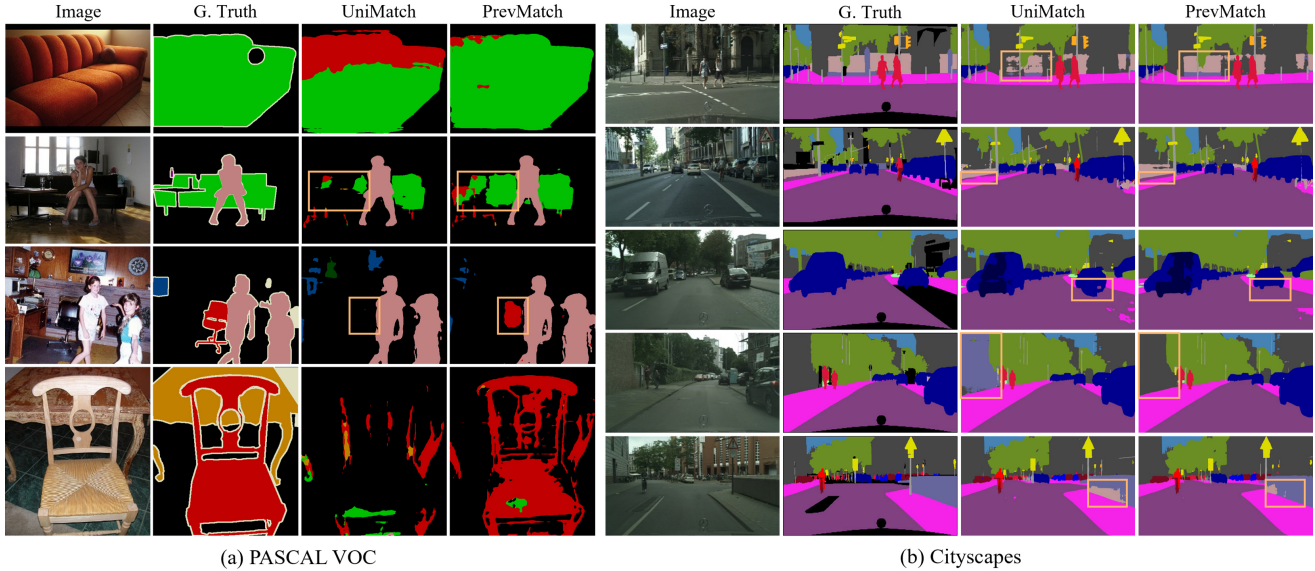


Fig. 3. Qualitative segmentation results on (a) Pascal VOC with a 92-label partition using a ResNet-50 encoder and (b) Cityscapes with a 1/16 label partition using a ResNet-101 encoder.

TABLE 10

Class-wise IoU scores for Pascal VOC with a 92-label partition using a ResNet-50 encoder.  $\Delta$  indicates the difference between the PrevMatch and baseline UniMatch performances.

	backgr.	airplane	bicycle	bird	boat	bottle	bus	car	cat	chair	cow	table	dog	horse	m.bike	person	plant	sheep	sofa	train	tv
UniMatch	91	84	59	89	71	68	92	80	88	8	88	55	85	85	75	80	54	82	33	80	64
PrevMatch	93	84	61	87	71	68	93	84	89	21	89	57	84	86	77	82	51	82	46	84	58
$\Delta$	2	0	2	-2	0	0	1	4	1	13	1	2	-1	1	2	2	-3	0	13	4	-6

TABLE 11

Class-wise IoU scores for Cityscapes with a 1/8 label partition using a ResNet-101 encoder.

	road	sidewalk	build.	wall	fence	pole	t.light	t.sign	veget.	terrain	sky	person	rider	car	truck	bus	train	m.cycle	bicycle
UniMatch	98	82	92	56	60	62	71	79	92	60	95	82	63	95	83	87	79	68	77
PrevMatch	98	84	92	60	63	63	71	80	92	63	95	82	64	95	83	88	81	69	77
$\Delta$	0	2	0	4	3	1	0	1	0	3	0	0	1	0	0	1	2	1	0

**Training Stability of Poorly Behaved Classes.** To further explore the catastrophic forgetting problem in poorly behaved classes, we visualize changes in terms of pseudo-label accuracy and validation IoU scores during training, as depicted in Fig. 4. In the first row (chair class), the training curve of the baseline pseudo-label accuracy exhibits significant fluctuations, particularly showing a sudden sharp performance drop at approximately 50 epochs. Although the pseudo-label accuracy recovers slightly thereafter, the validation score does not. In the second row (sofa class), the training curve of the baseline exhibits more severe fluctuations and sharper and more drastic performance drops than in the first row. In contrast, the proposed method shows a smoother training curve without significant fluctuations in either category. This indicates that the proposed training procedure aids in achieving stable optimization for poorly behaved classes that suffer from the forgetting problem.

**Training Stability Across Different Label Partitions.** Fig. 5 illustrates the effect of the proposed method on the changes

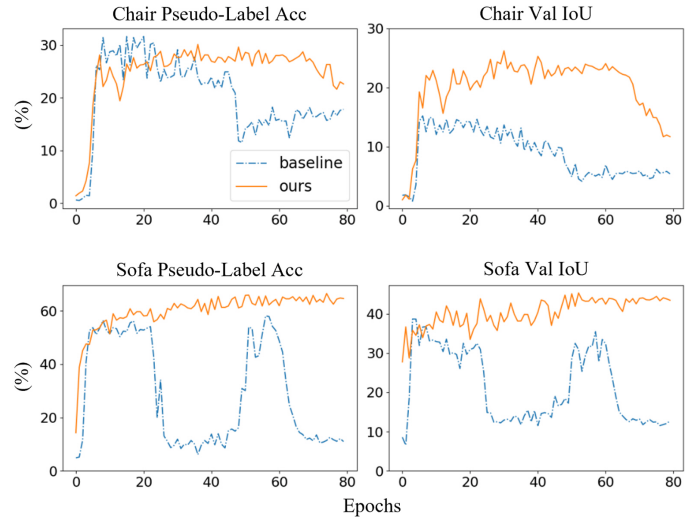


Fig. 4. Training curves for the chair and sofa classes, illustrating variations in pseudo-label pixel accuracy and validation IoU scores. The experiment is conducted on the 92-label partition of Pascal VOC.

in the validation scores throughout the training process. In fewer label settings (92 and 183), the baseline (blue) exhibits significant fluctuations in terms of performance compared to the proposed method (orange). Moreover, when considering the epoch that achieves the best performance, the baseline method struggles to converge consistently across epochs and tends to become trapped in local minima prematurely. This issue is particularly pronounced in scenarios with fewer labels. In contrast, the proposed method consistently converges across epochs without significant fluctuations. Finally, the consistent outperformance of our method over the baseline across almost all training epochs in label partitions suggests that the positive effects of previous guidance outweigh any negative effects. Note that the positive and negative effects refer to the cases (3) and (2), respectively, described in the last paragraph of Section 3.2.

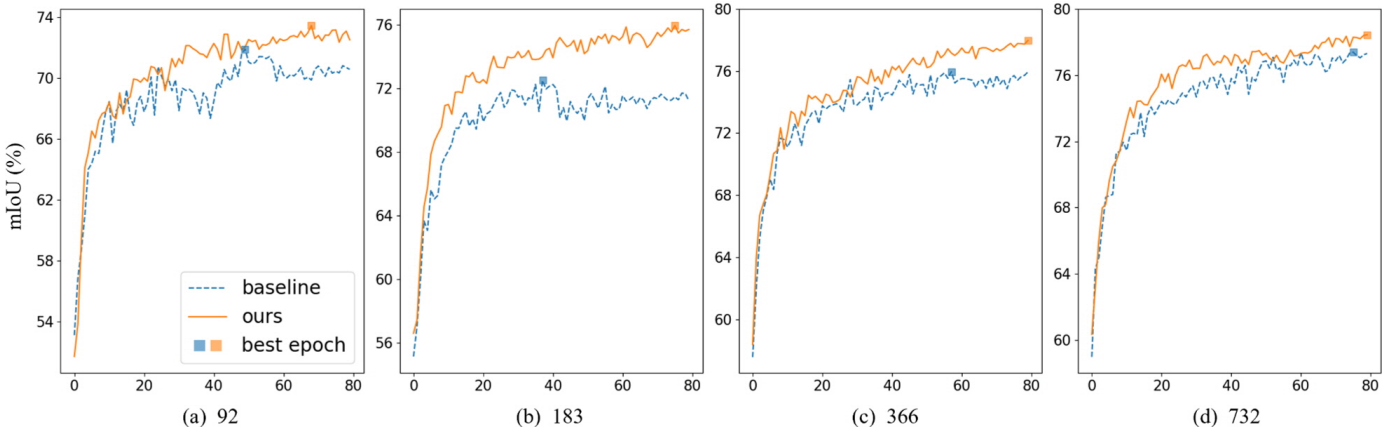


Fig. 5. Training curves for different label partition settings on Pascal VOC. The X- and Y-axes represent epochs and validation mIoU, respectively. The square symbol (■) denotes the epoch with the best performance.

TABLE 12

Comparison of time spent using existing methods with a ResNet-101 encoder. Training time per epoch and GPU memory usage were measured using the same environment (two A6000 GPUs) and hyperparameters, such as batch size, in a 92-label partition. We used the open-sourced code provided by the authors.

Method	#Trainable Networks	Training Time (m)	GPU Memory Usage (G)	Pascal		
				92	183	366
UniMatch	1	7.8	21.9	75.2	77.2	78.8
Diverse Co-T.	3	22.1	40.5	75.4	76.8	79.6
PS-MT	1	24.9	28.6	65.8	69.6	76.6
ours ( $K=1$ )	1	8.4	22.7	76.4	77.5	79.3
ours ( $K=3$ )	1	9.1	22.7	77.0	78.5	79.6

The results presented in this subsection suggest the following implications: (1) Training with fewer labels leads to instability in pseudo-label predictions, particularly for poorly behaved classes. (2) The proposed training procedure aids in stabilizing pseudo-label predictions while mitigating the forgetting problem in poorly behaved classes. (3) In other words, leveraging previous knowledge helps alleviate the issues of tight coupling and catastrophic forgetting, which can hinder stable learning in semi-supervised segmentation settings.

#### 4.4.2 Efficiency Evaluation

To investigate the complexities of the proposed method, we measure the training time per epoch and GPU memory usage. In Table 12, Diverse Co-training, based on the co-training approach, slightly outperforms UniMatch, which operates on a single trainable network, in terms of performance. However, Diverse Co-training requires approximately three times more training time and twice as much memory, resulting in limited scalability. Moreover, PS-MT, a dual Mean Teacher-based method, requires training time comparable to that of Diverse Co-training due to its complex components, despite being a single trainable network. In contrast, the proposed method significantly outperforms existing methods, with a slight cost increase. In particular, PrevMatch ( $K=3$ ) outperforms UniMatch by 1.8% in terms of mIoU (92 label setting) while requiring only a slight increase in complexities in training time and GPU usage, suggesting that PrevMatch can efficiently provide diverse

pseudo-labels. Therefore, owing to its computational efficiency and the simplicity of its pipeline reusing the same inputs, the proposed method can be easily integrated into any semi-supervised learning method.

## 5 CONCLUSION AND FUTURE WORK

In this work, we introduced the PrevMatch framework, which leverages temporal knowledge obtained during training to efficiently address the issues of tight coupling and confirmation bias that impede stable semi-supervised learning. The main contributions of PrevMatch include revisiting the use of temporal knowledge and maximizing its effectiveness. Specifically, we directly utilized previous models to provide additional pseudo-label guidance, referred to as previous guidance, to the student network. In addition, we developed a highly randomized ensemble strategy that enhances the reliability and diversity of the previous guidance while minimizing the increase in computational complexity. Experiments were conducted on four benchmark semantic segmentation datasets, revealing that PrevMatch significantly outperforms existing state-of-the-art methods across different evaluation protocols. Furthermore, our findings indicate that leveraging temporal knowledge facilitates stable optimization, particularly for classes that exhibit poor performance and fluctuations. Finally, the computational efficiency and compatibility of the proposed method facilitate its seamless integration into recent semi-supervised semantic segmentation methods.

In future work, we will investigate the capability of PrevMatch to address the domain adaptation problem. This problem poses a more challenging self-training task due to domain discrepancies between the labeled and unlabeled images, a commonly encountered problem in real-world applications. In addition, we observed a phenomenon where significant fluctuations in pseudo-label accuracy for several classes negatively affect generalization ability. For instance, pseudo-label accuracy recovers slightly after a sharp drop in performance; however, the validation score does not. Although the proposed method has shown that it can mitigate these issues, a more in-depth investigation is required for scenarios involving many classes and imbalanced distributions, such as the COCO and ADE20K datasets. Therefore,

we intend to explore this phenomenon extensively across different classes, in terms of the relationship between training instability and generalization ability.

## ACKNOWLEDGMENTS

This research was supported by Brain Korea 21 FOUR. This research was also supported by Korea University Grant (K2403371) and Korea TechnoComplex Foundation Grant (R2112653).

## REFERENCES

- [1] E. Shelhamer, J. Long, and T. Darrell, "Fully convolutional networks for semantic segmentation," *IEEE Transactions on Pattern Analysis and Machine Intelligence*, vol. 39, no. 4, pp. 640–651, 2017.
- [2] L.-C. Chen, G. Papandreou, I. Kokkinos, K. Murphy, and A. L. Yuille, "Deepplab: Semantic image segmentation with deep convolutional nets, atrous convolution, and fully connected crfs," *IEEE transactions on pattern analysis and machine intelligence*, vol. 40, no. 4, pp. 834–848, 2017.
- [3] L.-C. Chen, Y. Zhu, G. Papandreou, F. Schroff, and H. Adam, "Encoder-decoder with atrous separable convolution for semantic image segmentation," in *Proceedings of the European conference on computer vision (ECCV)*, 2018, pp. 801–818.
- [4] V. Badrinarayanan, A. Kendall, and R. Cipolla, "Segnet: A deep convolutional encoder-decoder architecture for image segmentation," *IEEE transactions on pattern analysis and machine intelligence*, vol. 39, no. 12, pp. 2481–2495, 2017.
- [5] J. Wang, K. Sun, T. Cheng, B. Jiang, C. Deng, Y. Zhao, D. Liu, Y. Mu, M. Tan, X. Wang *et al.*, "Deep high-resolution representation learning for visual recognition," *IEEE transactions on pattern analysis and machine intelligence*, vol. 43, no. 10, pp. 3349–3364, 2020.
- [6] E. Xie, W. Wang, Z. Yu, A. Anandkumar, J. M. Alvarez, and P. Luo, "Segformer: Simple and efficient design for semantic segmentation with transformers," *Advances in neural information processing systems*, vol. 34, pp. 12 077–12 090, 2021.
- [7] W. Wang, J. Dai, Z. Chen, Z. Huang, Z. Li, X. Zhu, X. Hu, T. Lu, L. Lu, H. Li *et al.*, "Internimage: Exploring large-scale vision foundation models with deformable convolutions," in *Proceedings of the IEEE/CVF Conference on Computer Vision and Pattern Recognition*, 2023, pp. 14 408–14 419.
- [8] D.-P. Fan, G.-P. Ji, T. Zhou, G. Chen, H. Fu, J. Shen, and L. Shao, "Pranet: Parallel reverse attention network for polyp segmentation," in *International conference on medical image computing and computer-assisted intervention*. Springer, 2020, pp. 263–273.
- [9] W. Shin, M. S. Lee, and S. W. Han, "Comma: propagating complementary multi-level aggregation network for polyp segmentation," *Applied Sciences*, vol. 12, no. 4, p. 2114, 2022.
- [10] A. Milioto and C. Stachniss, "Bonnet: An open-source training and deployment framework for semantic segmentation in robotics using cnns," in *2019 international conference on robotics and automation (ICRA)*. IEEE, 2019, pp. 7094–7100.
- [11] M. S. Lee, W. Shin, and S. W. Han, "Tracer: Extreme attention guided salient object tracing network (student abstract)," in *Proceedings of the AAAI conference on artificial intelligence*, vol. 36, no. 11, 2022, pp. 12 993–12 994.
- [12] Q. Hu, B. Yang, L. Xie, S. Rosa, Y. Guo, Z. Wang, N. Trigoni, and A. Markham, "Learning semantic segmentation of large-scale point clouds with random sampling," *IEEE Transactions on Pattern Analysis and Machine Intelligence*, vol. 44, no. 11, pp. 8338–8354, 2021.
- [13] M. S. Lee, S. W. Yang, and S. W. Han, "Gaia: Graphical information gain based attention network for weakly supervised point cloud semantic segmentation," in *Proceedings of the IEEE/CVF Winter Conference on Applications of Computer Vision*, 2023, pp. 582–591.
- [14] Y. Grandvalet and Y. Bengio, "Semi-supervised learning by entropy minimization," *Advances in neural information processing systems*, vol. 17, 2004.
- [15] C. Rosenberg, M. Hebert, and H. Schneiderman, "Semi-supervised self-training of object detection models," 2005.
- [16] D.-H. Lee *et al.*, "Pseudo-label: The simple and efficient semi-supervised learning method for deep neural networks," in *Workshop on challenges in representation learning, ICML*, vol. 3, no. 2. Atlanta, 2013, p. 896.
- [17] E. Arazo, D. Ortego, P. Albert, N. E. O'Connor, and K. McGuinness, "Pseudo-labeling and confirmation bias in deep semi-supervised learning," in *2020 International joint conference on neural networks (IJCNN)*. IEEE, 2020, pp. 1–8.
- [18] P. Cascante-Bonilla, F. Tan, Y. Qi, and V. Ordonez, "Curriculum labeling: Revisiting pseudo-labeling for semi-supervised learning," in *Proceedings of the AAAI conference on artificial intelligence*, vol. 35, no. 8, 2021, pp. 6912–6920.
- [19] B. Chen, J. Jiang, X. Wang, P. Wan, J. Wang, and M. Long, "Debiased self-training for semi-supervised learning," *Advances in Neural Information Processing Systems*, vol. 35, pp. 32 424–32 437, 2022.
- [20] T. Zhou, S. Wang, and J. Bilmes, "Time-consistent self-supervision for semi-supervised learning," in *International Conference on Machine Learning*. PMLR, 2020, pp. 11 523–11 533.
- [21] L. Yang, W. Zhuo, L. Qi, Y. Shi, and Y. Gao, "St++: Make self-training work better for semi-supervised semantic segmentation," in *Proceedings of the IEEE/CVF Conference on Computer Vision and Pattern Recognition*, 2022, pp. 4268–4277.
- [22] M. Sajjadi, M. Javanmardi, and T. Tasdizen, "Regularization with stochastic transformations and perturbations for deep semi-supervised learning," *Advances in neural information processing systems*, vol. 29, 2016.
- [23] S. Laine and T. Aila, "Temporal ensembling for semi-supervised learning," *arXiv preprint arXiv:1610.02242*, 2016.
- [24] T. Miyato, S.-i. Maeda, M. Koyama, and S. Ishii, "Virtual adversarial training: a regularization method for supervised and semi-supervised learning," *IEEE transactions on pattern analysis and machine intelligence*, vol. 41, no. 8, pp. 1979–1993, 2018.
- [25] Q. Xie, Z. Dai, E. Hovy, T. Luong, and Q. Le, "Unsupervised data augmentation for consistency training," *Advances in neural information processing systems*, vol. 33, pp. 6256–6268, 2020.
- [26] A. Tarvainen and H. Valpola, "Mean teachers are better role models: Weight-averaged consistency targets improve semi-supervised deep learning results," *Advances in neural information processing systems*, vol. 30, 2017.
- [27] Z. Ke, D. Wang, Q. Yan, J. Ren, and R. W. Lau, "Dual student: Breaking the limits of the teacher in semi-supervised learning," in *Proceedings of the IEEE/CVF international conference on computer vision*, 2019, pp. 6728–6736.
- [28] X. Chen, Y. Yuan, G. Zeng, and J. Wang, "Semi-supervised semantic segmentation with cross pseudo supervision," in *Proceedings of the IEEE/CVF Conference on Computer Vision and Pattern Recognition*, 2021, pp. 2613–2622.
- [29] Y. Li, X. Wang, L. Yang, L. Feng, W. Zhang, and Y. Gao, "Diverse cotraining makes strong semi-supervised segmentor," *arXiv preprint arXiv:2308.09281*, 2023.
- [30] Y. Liu, Y. Tian, Y. Chen, F. Liu, V. Belagiannis, and G. Carneiro, "Perturbed and strict mean teachers for semi-supervised semantic segmentation," in *Proceedings of the IEEE/CVF Conference on Computer Vision and Pattern Recognition*, 2022, pp. 4258–4267.
- [31] J. Na, J.-W. Ha, H. J. Chang, D. Han, and W. Hwang, "Switching temporary teachers for semi-supervised semantic segmentation," *arXiv preprint arXiv:2310.18640*, 2023.
- [32] L. Yang, L. Qi, L. Feng, W. Zhang, and Y. Shi, "Revisiting weak-to-strong consistency in semi-supervised semantic segmentation," in *Proceedings of the IEEE/CVF Conference on Computer Vision and Pattern Recognition*, 2023, pp. 7236–7246.
- [33] L. Hoyer, D. J. Tan, M. F. Naeem, L. Van Gool, and F. Tombari, "Semivl: Semi-supervised semantic segmentation with vision-language guidance," *arXiv preprint arXiv:2311.16241*, 2023.
- [34] K. Sohn, D. Berthelot, N. Carlini, Z. Zhang, H. Zhang, C. A. Raffel, E. D. Cubuk, A. Kurakin, and C.-L. Li, "Fixmatch: Simplifying semi-supervised learning with consistency and confidence," *Advances in neural information processing systems*, vol. 33, pp. 596–608, 2020.
- [35] Y. Zou, Z. Zhang, H. Zhang, C.-L. Li, X. Bian, J.-B. Huang, and T. Pfister, "Pseudoseg: Designing pseudo labels for semantic segmentation," *arXiv preprint arXiv:2010.09713*, 2020.
- [36] Q. Xie, M.-T. Luong, E. Hovy, and Q. V. Le, "Self-training with noisy student improves imagenet classification," in *Proceedings of the IEEE/CVF conference on computer vision and pattern recognition*, 2020, pp. 10 687–10 698.
- [37] Y. Ouali, C. Hudelot, and M. Tami, "An overview of deep semi-supervised learning," *arXiv preprint arXiv:2006.05278*, 2020.

- [38] G. French, S. Laine, T. Aila, M. Mackiewicz, and G. Finlayson, "Semi-supervised semantic segmentation needs strong, varied perturbations," *arXiv preprint arXiv:1906.01916*, 2019.
- [39] Z. Zhao, L. Yang, S. Long, J. Pi, L. Zhou, and J. Wang, "Augmentation matters: A simple-yet-effective approach to semi-supervised semantic segmentation," in *Proceedings of the IEEE/CVF Conference on Computer Vision and Pattern Recognition*, 2023, pp. 11 350–11 359.
- [40] Z. Zhao, S. Long, J. Pi, J. Wang, and L. Zhou, "Instance-specific and model-adaptive supervision for semi-supervised semantic segmentation," in *Proceedings of the IEEE/CVF Conference on Computer Vision and Pattern Recognition*, 2023, pp. 23 705–23 714.
- [41] S. Yun, D. Han, S. J. Oh, S. Chun, J. Choe, and Y. Yoo, "Cutmix: Regularization strategy to train strong classifiers with localizable features," in *Proceedings of the IEEE/CVF international conference on computer vision*, 2019, pp. 6023–6032.
- [42] V. Olsson, W. Tranheden, J. Pinto, and L. Svensson, "Classmix: Segmentation-based data augmentation for semi-supervised learning," in *Proceedings of the IEEE/CVF winter conference on applications of computer vision*, 2021, pp. 1369–1378.
- [43] S. Qiao, W. Shen, Z. Zhang, B. Wang, and A. Yuille, "Deep co-training for semi-supervised image recognition," in *Proceedings of the european conference on computer vision (eccv)*, 2018, pp. 135–152.
- [44] Y. Ouali, C. Hudelot, and M. Tami, "Semi-supervised semantic segmentation with cross-consistency training," in *Proceedings of the IEEE/CVF Conference on Computer Vision and Pattern Recognition*, 2020, pp. 12 674–12 684.
- [45] D. Filipiak, P. Tempczyk, and M. Cygan, "n-cps: Generalising cross pseudo supervision to n networks for semi-supervised semantic segmentation," *arXiv preprint arXiv:2112.07528*, 2021.
- [46] J. Fan, B. Gao, H. Jin, and L. Jiang, "Ucc: Uncertainty guided cross-head co-training for semi-supervised semantic segmentation," in *Proceedings of the IEEE/CVF conference on computer vision and pattern recognition*, 2022, pp. 9947–9956.
- [47] Z. Wang, Z. Zhao, X. Xing, D. Xu, X. Kong, and L. Zhou, "Conflict-based cross-view consistency for semi-supervised semantic segmentation," in *Proceedings of the IEEE/CVF Conference on Computer Vision and Pattern Recognition*, 2023, pp. 19 585–19 595.
- [48] D. Berthelot, N. Carlini, I. Goodfellow, N. Papernot, A. Oliver, and C. A. Raffel, "Mixmatch: A holistic approach to semi-supervised learning," *Advances in neural information processing systems*, vol. 32, 2019.
- [49] Z. Feng, Q. Zhou, Q. Gu, X. Tan, G. Cheng, X. Lu, J. Shi, and L. Ma, "Dmt: Dynamic mutual training for semi-supervised learning," *Pattern Recognition*, vol. 130, p. 108777, 2022.
- [50] A. Rasmus, M. Berglund, M. Honkala, H. Valpola, and T. Raiko, "Semi-supervised learning with ladder networks," *Advances in neural information processing systems*, vol. 28, 2015.
- [51] E. D. Cubuk, B. Zoph, J. Shlens, and Q. V. Le, "Randaugment: Practical automated data augmentation with a reduced search space," in *Proceedings of the IEEE/CVF conference on computer vision and pattern recognition workshops*, 2020, pp. 702–703.
- [52] N. Souly, C. Spampinato, and M. Shah, "Semi-supervised semantic segmentation using generative adversarial network," in *Proceedings of the IEEE international conference on computer vision*, 2017, pp. 5688–5696.
- [53] S. Mittal, M. Tatarchenko, and T. Brox, "Semi-supervised semantic segmentation with high-and low-level consistency," *IEEE transactions on pattern analysis and machine intelligence*, vol. 43, no. 4, pp. 1369–1379, 2019.
- [54] I. Goodfellow, J. Pouget-Abadie, M. Mirza, B. Xu, D. Warde-Farley, S. Ozair, A. Courville, and Y. Bengio, "Generative adversarial nets," *Advances in neural information processing systems*, vol. 27, 2014.
- [55] Z. Ke, D. Qiu, K. Li, Q. Yan, and R. W. Lau, "Guided collaborative training for pixel-wise semi-supervised learning," in *Computer Vision—ECCV 2020: 16th European Conference, Glasgow, UK, August 23–28, 2020, Proceedings, Part XIII 16*. Springer, 2020, pp. 429–445.
- [56] H. Hu, F. Wei, H. Hu, Q. Ye, J. Cui, and L. Wang, "Semi-supervised semantic segmentation via adaptive equalization learning," *Advances in Neural Information Processing Systems*, vol. 34, pp. 22 106–22 118, 2021.
- [57] H. Xu, L. Liu, Q. Bian, and Z. Yang, "Semi-supervised semantic segmentation with prototype-based consistency regularization," *Advances in Neural Information Processing Systems*, vol. 35, pp. 26 007–26 020, 2022.
- [58] J. Ma, C. Wang, Y. Liu, L. Lin, and G. Li, "Enhanced soft label for semi-supervised semantic segmentation," in *Proceedings of the IEEE/CVF International Conference on Computer Vision*, 2023, pp. 1185–1195.
- [59] C. Liang, W. Wang, J. Miao, and Y. Yang, "Logic-induced diagnostic reasoning for semi-supervised semantic segmentation," in *Proceedings of the IEEE/CVF International Conference on Computer Vision*, 2023, pp. 16 197–16 208.
- [60] S. Fan, F. Zhu, Z. Feng, Y. Lv, M. Song, and F.-Y. Wang, "Conservative-progressive collaborative learning for semi-supervised semantic segmentation," *IEEE Transactions on Image Processing*, 2023.
- [61] W. Feng, Y. Wang, L. Ma, Y. Yuan, and C. Zhang, "Temporal knowledge consistency for unsupervised visual representation learning," in *Proceedings of the IEEE/CVF International Conference on Computer Vision*, 2021, pp. 10 170–10 180.
- [62] G. Huang, Y. Li, G. Pleiss, Z. Liu, J. E. Hopcroft, and K. Q. Weinberger, "Snapshot ensembles: Train 1, get m for free," *arXiv preprint arXiv:1704.00109*, 2017.
- [63] C. Wang, Q. Yang, R. Huang, S. Song, and G. Huang, "Efficient knowledge distillation from model checkpoints," *Advances in Neural Information Processing Systems*, vol. 35, pp. 607–619, 2022.
- [64] M. McCloskey and N. J. Cohen, "Catastrophic interference in connectionist networks: The sequential learning problem," in *Psychology of learning and motivation*. Elsevier, 1989, vol. 24, pp. 109–165.
- [65] J. Kirkpatrick, R. Pascanu, N. Rabinowitz, J. Veness, G. Desjardins, A. A. Rusu, K. Milan, J. Quan, T. Ramalho, A. Grabska-Barwinska et al., "Overcoming catastrophic forgetting in neural networks," *Proceedings of the national academy of sciences*, vol. 114, no. 13, pp. 3521–3526, 2017.
- [66] M. Everingham, L. Van Gool, C. K. Williams, J. Winn, and A. Zisserman, "The pascal visual object classes (voc) challenge," *International journal of computer vision*, vol. 88, pp. 303–338, 2010.
- [67] Y. Wang, H. Wang, Y. Shen, J. Fei, W. Li, G. Jin, L. Wu, R. Zhao, and X. Le, "Semi-supervised semantic segmentation using unreliable pseudo-labels," in *Proceedings of the IEEE/CVF Conference on Computer Vision and Pattern Recognition*, 2022, pp. 4248–4257.
- [68] M. Cordts, M. Omran, S. Ramos, T. Rehfeld, M. Enzweiler, R. Benenson, U. Franke, S. Roth, and B. Schiele, "The cityscapes dataset for semantic urban scene understanding," in *Proceedings of the IEEE conference on computer vision and pattern recognition*, 2016, pp. 3213–3223.
- [69] T.-Y. Lin, M. Maire, S. Belongie, J. Hays, P. Perona, D. Ramanan, P. Dollár, and C. L. Zitnick, "Microsoft coco: Common objects in context," in *Computer Vision—ECCV 2014: 13th European Conference, Zurich, Switzerland, September 6–12, 2014, Proceedings, Part V 13*. Springer, 2014, pp. 740–755.
- [70] B. Zhou, H. Zhao, X. Puig, S. Fidler, A. Barriuso, and A. Torralba, "Scene parsing through ade20k dataset," in *Proceedings of the IEEE conference on computer vision and pattern recognition*, 2017, pp. 633–641.
- [71] K. He, X. Zhang, S. Ren, and J. Sun, "Deep residual learning for image recognition," in *Proceedings of the IEEE conference on computer vision and pattern recognition*, 2016, pp. 770–778.
- [72] F. Chollet, "Xception: Deep learning with depthwise separable convolutions," in *Proceedings of the IEEE conference on computer vision and pattern recognition*, 2017, pp. 1251–1258.
- [73] Y. Zhong, B. Yuan, H. Wu, Z. Yuan, J. Peng, and Y.-X. Wang, "Pixel contrastive-consistent semi-supervised semantic segmentation," in *Proceedings of the IEEE/CVF International Conference on Computer Vision*, 2021, pp. 7273–7282.
- [74] S. Liu, S. Zhi, E. Johns, and A. J. Davison, "Bootstrapping semantic segmentation with regional contrast," *arXiv preprint arXiv:2104.04465*, 2021.
- [75] Y. Jin, J. Wang, and D. Lin, "Semi-supervised semantic segmentation via gentle teaching assistant," *Advances in Neural Information Processing Systems*, vol. 35, pp. 2803–2816, 2022.
- [76] X. Wang, B. Zhang, L. Yu, and J. Xiao, "Hunting sparsity: Density-guided contrastive learning for semi-supervised semantic segmentation," in *Proceedings of the IEEE/CVF Conference on Computer Vision and Pattern Recognition*, 2023, pp. 3114–3123.
- [77] X. Lai, Z. Tian, L. Jiang, S. Liu, H. Zhao, L. Wang, and J. Jia, "Semi-supervised semantic segmentation with directional context-aware consistency," in *Proceedings of the IEEE/CVF Conference on Computer Vision and Pattern Recognition*, 2021, pp. 1205–1214.
- [78] P. Qiao, Z. Wei, Y. Wang, Z. Wang, G. Song, F. Xu, X. Ji, C. Liu, and J. Chen, "Fuzzy positive learning for semi-supervised semantic

segmentation,” in *Proceedings of the IEEE/CVF Conference on Computer Vision and Pattern Recognition*, 2023, pp. 15 465–15 474.

- [79] L. Wu, L. Fang, X. He, M. He, J. Ma, and Z. Zhong, “Querying labeled for unlabeled: Cross-image semantic consistency guided semi-supervised semantic segmentation,” *IEEE Transactions on Pattern Analysis and Machine Intelligence*, 2023.
- [80] Y. Fang, F. Zhu, B. Cheng, L. Liu, Y. Zhao, and Y. Wei, “Locating noise is halfway denoising for semi-supervised segmentation,” in *Proceedings of the IEEE/CVF International Conference on Computer Vision*, 2023, pp. 16 612–16 622.



**Wooseok Shin** received his B.S. degree in Industrial and Information Systems Engineering from Seoul National University of Science and Technology, Seoul, Republic of Korea, in 2020. He is currently pursuing his Ph.D. degree at the School of Industrial and Management Engineering, Korea University, Seoul. He has authored and co-authored scientific articles at top venues, including ICML, INTERSPEECH, ICASSP, and AAAI. His research interests include developing learning methodologies for dense prediction

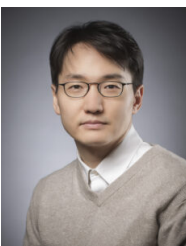
tasks in computer vision and speech processing.



**Hyun Joon Park** received his B.S. degree in Industrial Engineering from Hongik University, Seoul, South Korea, in 2020. He is currently working toward his Ph.D. degree in School of Industrial and Management Engineering, Korea University, Seoul. His research interests include speech enhancement, voice conversion, and speech synthesis, using artificial intelligence.



**Jin Sob Kim** received his B.S. degree in computer engineering from Hongik University, Seoul, South Korea, in 2021. He is currently working toward his Ph.D. degree in time-spatial data processing and speech-processing network architectures at the School of Industrial and Management Engineering, Korea University, Seoul. His research interests include spatio-temporal data and signal processing deep learning architectures, and network training strategies.



**Sung Won Han** received his M.S. degrees in operations research, statistics, and mathematics from Georgia Institute of Technology, in 2006, 2007, and 2010, respectively, and his Ph.D. degree from the School of Industrial and Systems Engineering, Georgia Institute of Technology. He worked as a senior research scientist with the Division of Biostatistics, School of Medicine, New York University, and as a postdoctoral researcher with the Department of Biostatistics and Epidemiology/Center for Clinical Epidemiol-

ogy and Biostatistics, School of Medicine, University of Pennsylvania. He works currently as a professor at the School of Industrial and Management Engineering, Korea University. His research interests include probabilistic graphical models, network analysis, machine learning, and deep learning.